Experimental determination of the ionization energy of IO(XÂ²/Î ââ) and estmations of Î{sub f}HÂ°â(IO{sup +}) and PA(IO)

ARTICLE · JANUARY 1996

DOI: 10.1021/jp952405p

7 AUTHORS, INCLUDING:

Paul S. Monks
University of Leicester
295 PUBLICATIONS **5,503** CITATIONS
SEE PROFILE

Robert Huie
National Institute of Standards and Technolo…
192 PUBLICATIONS **7,943** CITATIONS
SEE PROFILE

Experimental Determination of the Ionization Energy of IO($X^2\Pi_{3/2}$) and Estimations of $\Delta_f H°_0(IO^+)$ and PA(IO)

Zhengyu Zhang

Brookhaven National Laboratory, Bldg. 815, P.O. Box 5000, Upton, New York 11973-5000

Paul S. Monks[†] and Louis J. Stief*

Laboratory for Extraterrestrial Physics (Code 690), NASA/Goddard Space Flight Center, Greenbelt, Maryland 20771

Joel F. Liebman

Department of Chemistry and Biochemistry, University of Maryland Baltimore County, Baltimore, Maryland 21228-5398

Robert E. Huie

Chemical Kinetics and Thermodynamics Division, National Institute of Standards and Technology, Gaithersburg, Maryland 20899

Szu-Cherng Kuo and R. Bruce Klemm*

Brookhaven National Laboratory, Bldg. 815, P.O. Box 5000, Upton, New York 11973-5000

Received: August 16, 1995[⊗]

Photoionization efficiency (PIE) spectra of IO($X^2\Pi_i$) were measured over the wavelength range $\lambda = 115.0-130.0$ nm and in the ionization threshold region $\lambda = 126.0-130.0$ nm, using a discharge flow-photoionization mass spectrometer apparatus coupled to a synchrotron radiation source. Iodine oxide was generated by the reactions of O(^{3}P) atoms with I_2 and CF_3I. The PIE spectra displayed step-function behavior. From the half-rise point of the initial step, a value of $9.73_5 \pm 0.01_7$ eV was obtained for the adiabatic ionization energy (IE) of IO, corresponding to the $IO^+(X^3\Sigma^-) \leftarrow IO(X^2\Pi_{3/2})$ transition. As this appears to be the first experimental determination of IE(IO), a trend analysis has been employed to provide further insight into the experimentally derived value. The separation between the first two steps in the PIE spectrum (which might be perturbed slightly due to autoionization) was used to derive the vibrational spacing of the cation, 1060 ± 160 cm^{-1}. A Rydberg progression, presumably converging to the excited $^1\Delta$ state of the cation, has a convergence limit that lies 0.596 eV above the ground state of the cation. A selected value for the bond dissociation energy of IO, $D°_0(IO) = 226$ kJ mol^{-1}, leads to $\Delta_f H°_0(IO) = 128 \pm 4$ kJ mol^{-1}. From this value for the heat of formation of IO, estimates are made for $\Delta_f H°_0(IO^+)$, $\Delta_f H°_0(HOI)$ and the proton affinity of IO.

Introduction

Recent speculation on the role of halogens in stratospheric ozone depletion has centered on the role of iodine compounds.[1] As little as 1 ppt of iodocarbons could have a significant effect on ozone levels in the lower stratosphere at mid-latitudes.[1] Solomon et al.[2] have shown that, for a given chemical scheme, the ozone destruction efficiency of iodine released into the stratosphere near 15−20 km would be more than 1000 times that of a similar amount of chlorine. The reason for this increased interest in I compounds is due to serious consideration of CF_3I as a replacement for halon fire suppressants, particularly CF_3Br.[2−4] By analogy with proposed mechanisms for the flame inhibition activity of CF_3Br,[3−5] it might be expected that CF_3I will also be chemically active in flames.

Iodine oxide, IO, is an important species in the atmospheric[6] and combustion[7] chemistry of iodine species. An accurate value for its heat of formation is essential in understanding the thermochemistry of reactions involving IO. However, unlike the situation with regard to the other halogen oxides, there is a remarkable lack of reliable thermodynamic data for IO.[8] Although it was qualitatively observed *via* mass spectrometry over twenty years ago,[9a] IO has more recently been quantitatively monitored mass spectrometrically[9b,9c−11] and *via* laser induced fluorescence[11] in kinetic studies of IO as reactant and product. Since it was first observed in flame emission by Vaidya[12] in 1937, IO has been studied spectroscopically to determine values for its molecular constants[13−16] and bond energy[17−20] (and thence $\Delta_f H°_0(IO)$). The heat of formation has also been variously estimated in other studies.[21−25]

In contrast to the number of spectroscopic studies of IO, the only values for the ionization energy, IE(IO), have been estimated *via* trend analyses.[26,27] The ground-state electronic configuration of IO (by analogy with BrO and using Mulliken notation) is

$$...10\sigma^2\ 11\sigma^2\ 12\sigma^2\ 6\pi^4\ 7\pi^3$$

The lowest energy ionization of IO, using vacuum-ultraviolet

[†] NAS/NRC Resident Research Associate. Present address: School of Environmental Sciences, University of East Anglia, Norwich, NR4 7TJ, England.

* To whom correspondence should be addressed.

[⊗] Abstract published in *Advance ACS Abstracts,* December 1, 1995.

0022-3654/96/20100-0063$12.00/0

TABLE 1: Wavelength Thresholds and Ionization Energies for IO

nominal λ resolution[a] (nm)	nominal λ step (nm)	adiabatic threshold[b] (nm)	IE[c] (eV)	second step[d] (nm)	$[O_2]$ (molecule cm^{-3})	[I-source] (molecule cm^{-3})	P (Torr)	v (cm s^{-1})
0.23	0.20	127.30 ± 0.23	9.740 ± 0.018	125.60 ± 0.23	1.15(14)	1.19(12)[e]	4.24	1387
0.23	0.20	127.40 ± 0.23	9.732 ± 0.018	125.70 ± 0.23	1.99(14)	1.48(12)[e]	4.28	1371
0.23	0.10	127.30 ± 0.23	9.740 ± 0.018		1.15(14)	1.19(12)[e]	4.24	1387
0.23	0.10	127.25 ± 0.23	9.743 ± 0.018		1.15(14)	1.19(12)[e]	4.24	1387
0.23	0.10	127.35 ± 0.23	9.736 ± 0.018		7.76(13)	1.51(12)[e]	4.26	1392
0.23	0.10	127.35 ± 0.23	9.736 ± 0.018		7.76(13)	1.51(12)[e]	4.26	1392
0.23	0.10	127.45 ± 0.23	9.728 ± 0.018		7.76(13)	1.51(12)[e]	4.26	1392
0.12	0.05	127.35 ± 0.12	9.736 ± 0.009		8.83(13)	1.10(12)[e]	4.22	1394
0.14	0.20	127.40 ± 0.14	9.732 ± 0.011	125.70 ± 0.14	1.14(14)	2.20(14)[f]	4.14	1473
0.14	0.20	127.50 ± 0.14	9.724 ± 0.011	125.80 ± 0.14	1.93(14)	4.88(14)[f]	5.26	1607

[a] Full width at half-maximum (fwhm). [b] Onset of the $0 \leftarrow 0$ transition, determined from the half-rise point at the threshold for ionization. The uncertainty is conservatively estimated to be equal to (±) the resolution (fwhm). [c] Ionization energy. The uncertainties are conservatively estimated to be equal to (±) the resolution. The average value of 10 independent determinations is 9.73_5 eV with a standard deviation of $\pm 0.005_8$ eV and an estimated overall uncertainty of $\pm 0.01_7$ eV (which is 3 times the standard deviation, i.e., 3σ). [d] Onset of the $1 \leftarrow 0$ transition, determined from the half-rise point. The uncertainty is conservatively estimated to be equal to (±) the resolution (fwhm). The average value of four determinations of the vibrational spacing between the $0 \leftarrow 0$ and the $1 \leftarrow 0$ transitions is 1063 cm^{-1} with an estimated overall uncertainty of ±161 cm^{-1}. [e] IO produced *via* reaction 1, the I source was I_2. [f] IO produced *via* reaction 2, the I source was CF_3I.

(VUV) radiation of $\lambda > 105$ nm, is expected to originate from the 7π orbital, corresponding to the $IO^+(X^3\Sigma^-) \leftarrow IO(X^2\Pi_i)$ transition. In this study, which continues our photoionization investigations of XO species,[28] we present the first determination of the $IO(X^2\Pi_i)$ photoionization efficiency (PIE) spectrum and photoionization threshold from which the IE is derived. In addition, IE(IO) is discussed in terms of trends in the XO series (X = Cl, Br, I).

Experimental Section

Experiments were performed on a discharge flow-photoionization mass spectrometer (DF-PIMS) apparatus that is coupled to beamline U-11 at the National Synchrotron Light Source (NSLS) at Brookhaven National Laboratory. Details of the apparatus and experimental conditions have been thoroughly discussed in previous publications.[27−33] Briefly, IO radicals were produced in a Teflon lined flow tube reactor *via* reaction 1, with $[I_2] \approx 1.3 \times 10^{12}$ molecules cm^{-3}. Oxygen atoms were

$$O(^3P) + I_2 \rightarrow IO + I \qquad (1)$$

$$k_1(298\ K) = 1.4 \times 10^{-10}\ cm^3\ molecule^{-1}\ s^{-1}\ (ref\ 34)$$

produced by passing O_2 through a microwave discharge cavity at the upstream end of the flow tube (about 100 cm from the nozzle); the initial concentration of O_2 was about 1.0×10^{14} molecules cm^{-3}. The I_2 vapor was introduced through the tip of the sliding injector at a distance of ≈5 cm from the sampling nozzle. Experiments were conducted at ambient temperature ($T = 298 \pm 2$ K) and at a flow tube pressure of about 4 Torr with helium carrier gas. With the tip of the injector at 5 cm from the nozzle and a flow velocity of about 1400 cm s^{-1}, reaction 1 was about 95% complete within the available reaction time (3.6 ms).

IO was also generated *via* reaction 2, with $[CF_3I] \approx 3 \times$

$$O(^3P) + CF_3I \rightarrow IO + CF_3 \qquad (2)$$

$$k_2(298\ K) = 1.1 \times 10^{-11}\ cm^3\ molecule^{-1}\ s^{-1}\ (ref\ 35)$$

10^{14} molecules cm^{-3}. With the tip of the injector set at a distance of about 3 cm and a flow velocity of about 1500 cm s^{-1}, reaction 2 was ≥99% complete within the available reaction time (2 ms). The details of conditions used in the flow tube for reactions 1 and 2 are given in Table 1.

The gaseous mixture in the flow tube was sampled as a molecular beam into the sample chamber and subsequently into the photoionization source of the mass spectrometer. Ions were mass selected with an axially aligned quadrupole mass filter, detected with a channeltron/pulse preamplifier and thence counted for preset integration times. Measurements of photoionization efficiency (PIE) spectra, the ratio of ion counts to light intensity versus wavelength, were made using tunable VUV radiation at the NSLS. A monochromator with a normal incidence grating (1200 lines/mm) was used to disperse the VUV light[33] and a LiF filter ($\lambda \geq 103$ nm) was used to eliminate second- and higher-order radiation. The intensity of the VUV light was monitored *via* a sodium salicylate coated window with an attached photomultiplier tube. The monochromator slit width was varied between 380 and 750 μm to give a spectral bandwidth (fwhm) of 0.12−0.23 nm. The zero-order setting for calibration of the monochromator was adjusted to ±0.01 nm at the beginning and checked at the end of each filling of the VUV ring. Typically, variations between the beginning and ending settings of zero-order corresponded to variations in the wavelength calibration of ±0.05 nm or less.

The helium (MG Industries, 99.9999%) and oxygen (MG Industries, 99.999%) were used as supplied. Iodine vapor was taken from a degassed sample of the solid (Mallinckrodt, resublimed, AR) and subsequently diluted to about 0.04% (by volume) with helium. Trifluoromethyl iodide (Aldrich, 99%) was thoroughly outgassed at 77 K prior to use.

Results

As an example of the PIMS experiment, the PIE spectrum of the iodine atom was measured over the wavelength range of $\lambda = 117.0-121.0$ nm where the atomic iodine was generated *via* reaction 1. As shown in Figure 1, the onset of ionization at $\lambda = 118.65$ nm corresponds to IE(I) = 10.450 ± 0.020 eV, which is in excellent agreement with the recommended value of 10.451 eV.[36,37] This level of agreement indicates that the wavelength calibration, established by the location of zero order, is excellent.[31,32] The residual signal beyond the threshold ($\lambda = 119.0-121.0$ nm) is due to ion-pair formation from photodissociation of I_2, i.e., $I_2 + h\nu \rightarrow I^+ + I^-$, which has a threshold at $\lambda = 138.6$ nm.[38]

The PIE spectrum for IO, at $m/z = 143$, is shown in Figure 2 in the wavelength region of 115.0−130.0 nm at 0.1 nm intervals. Since the spin−orbit splitting is about 2091 cm^{-1},[16] the excited ground state, $IO(X^2\Pi_{1/2})$ will not be populated at $T = 298$ K; and thus the PIE spectrum is expected to reflect only

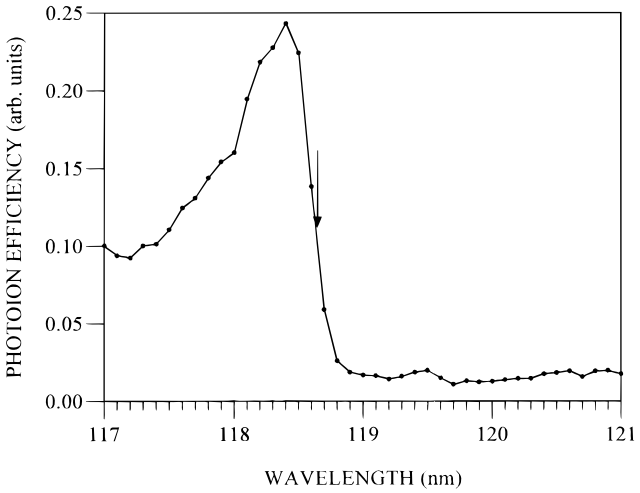

Figure 1. Photoionization efficiency spectrum of iodine atom (m/z = 127) between $\lambda = 117.0$ and 121.0 nm at a nominal resolution of 0.23 and 0.1 nm steps. Photoionization efficiency is ion counts divided by light intensity in arbitrary units. The arrow indicates the onset of ionization at $\lambda = 118.65$ nm (IE = 10.450 ± 0.020 eV where the uncertainty is conservatively estimated to be equal to (±) the resolution). $[I_2]_0 = 4.2 \times 10^{11}$ molecules cm^{-3}; $[O_2]_0 = 5.0 \times 10^{14}$ molecule cm^{-3}.

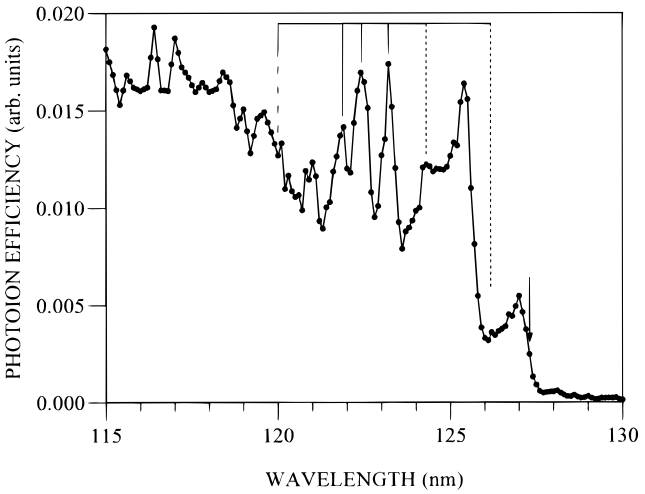

Figure 2. Photoionization efficiency spectrum of IO (m/z = 143) at a nominal resolution of about 0.23 and 0.10 nm steps between $\lambda = 115.0$ and 130.0 nm. Photoionization efficiency is ion counts divided by light intensity in arbitrary units. The arrow indicates the onset of ionization at 127.3 nm (IE = 9.74 ± 0.02 eV, where the uncertainty is conservatively estimated to be equal to (±) the resolution). The superposed lines indicate autoionization which presumably correlates with a Rydberg progression (126.2 nm/n^* = 5.18, 124.3 nm/n^* = 6.17, 123.2 nm/n^* = 7.12, 122.4 nm/n^* = 8.19, 121.9 nm/n^* = 9.19, where $n^* = (R/(\mathrm{IE} - \mathrm{E}_n))^{1/2}$ and R = 13.60539 eV) that converges to an excited state of the cation at 120.0 nm (10.33_2 eV). The first two members of the progression are indicated by dotted lines because they are so much weaker than the other members. $[I_2]_0 = 1.2 \times 10^{12}$ molecules cm^{-3}; $[O_2]_0 = 1.2 \times 10^{14}$ molecule cm^{-3}.

the transition $IO^+(X^3\Sigma^-) \leftarrow IO(X^2\Pi_{3/2})$. The spectrum should be free of perturbations caused by vibrational excitation because collisional deactivation is expected to occur rapidly.[27,32] The similarity in thresholds (see Table 1) and PIE spectra for IO that was produced by reactions 1 and 2 further support this claim since reaction 2 is not exothermic enough to populate $v'' = 1$ ($\Delta_r H°_{298} \approx -5$ kJ mol^{-1} and ω_e(IO) = 681 cm^{-1} (≈8 kJ mol^{-1})).[39] We also note that hot bands due to thermalized IO should not be apparent because the Boltzmann fraction of IO with $v'' = 1$ will be <4% at 298 K. As with PIE spectra of the other halogen oxides, BrO[28a] and FO,[28b] the spectrum of IO displays extensive structure, even at moderate resolution, which arises not only from the direct transition to the ion but also from a number of autoionizing Rydberg states. The ionic states that may contribute to the observed structure are the π^2 states $^3\Sigma^-$, $^1\Delta$ and $^1\Sigma^+$ (which have 7π character) and the $\pi^3\pi^3$ states $^1\Sigma^-$, $^3\Delta$, $^3\Sigma^+$, $^1\Sigma^+$, $^3\Sigma^-$, and $^1\Delta_i$ (which have mainly 6π character). Ionization in the threshold region, $\lambda = 125-128$ nm, exhibits step-function behavior with superimposed vibrational autoionization. The vibrational "steps" (at 127.3 and 125.7 nm) presumably correspond to transitions from the zero level of neutral IO ($X^2\Pi_{3/2}$) to the first two vibrational levels of the cation ($X^3\Sigma^-$). Although the superimposed autoionization may perturb both thresholds, the effect should be minor since autoionization should occur only at or above the thresholds. The vibrational spacing of IO^+ was calculated from four independent determinations (see Table 1) to be 1060 ± 160 cm^{-1}. This spacing is about 380 cm^{-1} larger than the vibrational frequency in the neutral (681 cm^{-1})[39] and is therefore consistent with the ejection of an antibonding electron. Within the additional autoionizing features, there is structure which is consistent with a Rydberg progression converging to an excited state of the cation at about 120 nm, or 0.596 eV above the ground state (see Figure 2). This convergence point corresponds to the energy difference between the ground state of the cation ($^3\Sigma^-$) and the first excited singlet state ($^1\Delta$) that has been calculated to be 0.624 eV (at the MCSCF level of theory).[40] However, this agreement may be fortuitous for several reasons. Since the transition to the second vibrational level of the $X^3\Sigma^-$ cation state is more intense than that to $v' = 0$, it is likely that the Rydberg progression also terminates at $v' = 1$ of the excited state of the cation. This would, therefore, place the convergence point of the progression between the $^1\Delta$ and the $^1\Sigma^+$ states rather than at the onset ($v' = 0$) of the $^1\Delta$ state. The apparent Rydberg progression is further complicated by the likely existence of additional progressions to other vibrational levels of the $^1\Delta$ state and transitions to the $^1\Sigma^+$ state that has been calculated to be only about 0.3 eV[40] higher in energy than the $^1\Delta$ state. Therefore, while the agreement between the apparent convergence point observed here and calculated energies of the first two excited states is gratifying, it is premature to make definitive assignments to these transitions.

To determine IE(IO) more precisely, a detailed examination near the threshold was carried out. The PIE spectrum is plotted in Figure 3A over the range $\lambda = 126.0-130.0$ nm at 0.1 nm intervals with a nominal resolution of 0.23 nm. The statistics were enhanced by accumulating multiple wavelength scans to improve the signal-to-background ratio. The threshold was analyzed by plotting the energy derivative of the IO PIE curve (Figure 3B), and the ionization energy was determined as the maximum of this derivative. Results from repeated measurements, listed in Table 1, are in excellent agreement and lead to an average value of $9.73_5 \pm 0.01_7$ eV for the adiabatic ionization energy of IO. The quoted uncertainty corresponds to 3 times the standard deviation ($\pm 0.005_8$ eV) of the 10 independent determinations. The present value for IE(IO) is listed in Table 2 along with ionization energies of the other XO radicals. Also included in Table 2 are electron affinities (EAs, ref 16) for XO, $\Delta_f H°_0$ for XO (refs 36 and 41), $\Delta_f H°_0$ for XO^+, and $D°_0$ for XO. The anomalous behavior of FO is particularly apparent in comparing the electron affinities or bond strengths of these species. The electron affinities are almost identical for FO and ClO but increase through the rest of the series. The behavior of the bond dissociation energies is even more dramatic, with the highest $D°_0$ belonging to ClO, the next to BrO, the lowest to FO, while IO is between BrO and FO.

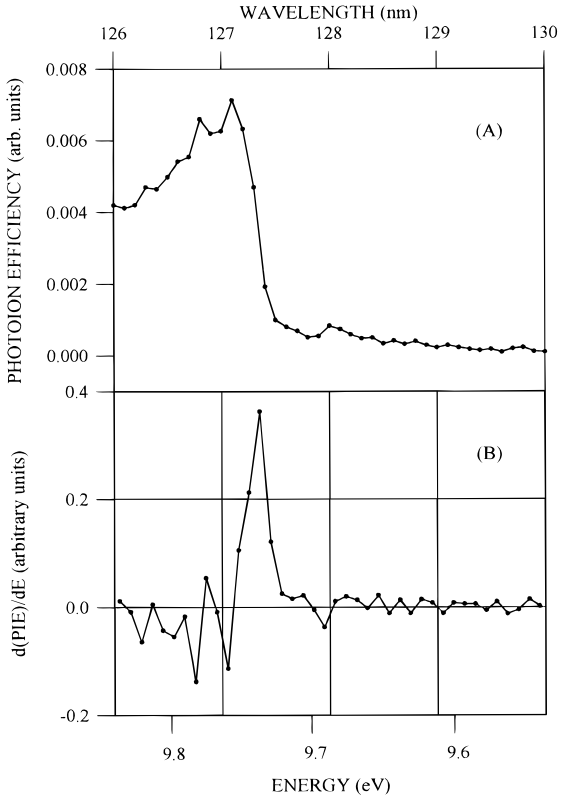

Figure 3. (A) Photoionization threshold region of IO ($m/z = 143$) at a nominal resolution of 0.23 and 0.1 nm steps between $\lambda = 126.0$ and 130.0 nm. (B) Energy derivative of (A). The maximum in the derivative is at $\lambda = 127.35$ nm ($9.73_6 \pm 0.01_8$ eV). $[I_2]_0 = 1.5 \times 10^{12}$ molecules cm^{-3}; $[O_2]_0 = 7.8 \times 10^{13}$ molecules cm^{-3}.

TABLE 2: Thermochemical Data for XO

compound	$D°_0$[a] (kJ mol^{-1})	$\Delta_f H°_0$(XO) (kJ mol^{-1})	$\Delta_f H°_0$(XO$^+$)[b] (kJ mol^{-1})	IE (eV)	EA[c] (eV)
FO	215.7	108.4[d]	1341.5	12.78[e]	2.272
ClO	265.4	101.0[d]	1157.5	10.95[f]	2.276
BrO	231.3	133.4[d]	1142.7	10.46[g]	2.353
IO	226[h]	≈128[i]	≈1067	9.735[j]	2.378

[a] Computed from $\Delta_f H°_0$ values for X and O listed in ref 41 and the values for XO listed here. [b] Sum of $\Delta_f H°_0$ and IE. [c] Reference 16 [d] Reference 41. [e] Reference 28b. [f] Reference 36. [g] Reference 28a. [h] Selected, see text and ref 8. [i] Derived from $D°_0$ and $\Delta_f H°_0$ values for X and O listed in ref 41. [j] This study.

Discussion

Trend Analysis. In an effort to understand the present result in the context of the observed value, we turn next to an estimation of the ionization energy of IO by considering IEs of related species. With IO, the bulk of the positive charge in IO$^+$ resides on the iodine atom. This is because both the ionization energy and electronegativity of the iodine atom are significantly less than the same quantities of the oxygen atom; and accordingly, it can be expected that measurements on ClO and BrO and their corresponding cations should provide insights for IO. In contrast, the relative ionization energy and electronegativity relationships for the X and O moieties are reversed for the lightest halogen atom, fluorine, such that data on FO and FO$^+$ are not appropriate for the present purpose; and thus, X is defined solely as Cl, Br and I. By using the ionization energy difference criteria, as discussed above, some common partner species (Z), for which the XZ is ionized essentially from the X moiety, are H, CH_3, C_2H_5, F, Cl, and OH. In the following statistical comparison between IE(XO) and IE(XZ), X = Cl and Br define a straight line; and thence IE(IZ) and the slope of the derived line are employed to derive IE(IO) for a given Z. Thus, the general equation is

TABLE 3: Ionization Energies of XZ Molecules and Derived Value for IE(IO)[a]

Z moiety	IE(XZ)[b] X = Cl	X = Br	X = I	derived IE(IO)
O	10.95	10.46[c]	**9.74**[d]	- - -
H	12.75	11.66	10.39	9.89
CH_3	11.22	10.54	9.54	9.74
C_2H_5	10.97	10.28	9.35	9.80
F	12.66[e]	11.77	10.54[e]	9.78
Cl	11.48	11.02[f]	10.09	9.47
OH	11.12[e]	10.63[g]	9.81[h]	9.64
- - -	12.967	11.814	10.451	9.88
				av 9.74 ± 0.15[i]

[a] Units are in electronvolts. [b] From ref 36 unless noted otherwise. [c] From ref 28a. [d] Present study, experimental value (see text). [e] From ref 42. [f] From ref 43. [g] Average of three values, from refs 26, 44, and 45. [h] From ref 27. [i] Mean value ± standard deviation (1σ).

$$\frac{\mathrm{IE(ClO)} - \mathrm{IE(BrO)}}{\mathrm{IE(ClZ)} - \mathrm{IE(BrZ)}} = \frac{\mathrm{IE(ClO)} - \mathrm{IE(IO)}}{\mathrm{IE(ClZ)} - \mathrm{IE(IZ)}} \qquad (3)$$

Rearranging and substituting the values for IE(ClO) and IE(BrO) listed in Table 3, one obtains

$$\mathrm{IE(IO)} = 10.95 - 0.49 \times \frac{\mathrm{IE(ClZ)} - \mathrm{IE(IZ)}}{\mathrm{IE(ClZ)} - \mathrm{IE(BrZ)}} \qquad (4)$$

In Table 3, ionization energy data (refs 26, 27, 28a, 36, and 42−45) are listed for use in this trend analysis along with the individual estimated values for IE(IO). The average value obtained for IE(IO) is 9.74 eV (with an uncertainty of ±0.15 eV at the 1σ level), which agrees remarkably well with the experimental value. The obvious advantage of the present trend analysis over the one employed by Ruscic and Berkowitz (R&B)[26] is the considerably larger dataset that is employed. Clearly, our potentially "crude" trend analysis, which relies heavily on the accuracy of the data in the literature and the perception of a trend, serves very effectively to bound the experimental result. This method may provide a means to estimate IEs of other species that are unknown or not firmly established.

To date, the only reported values for IE(IO) are estimates made by R&B[26] and Monks et al.[27] The estimation method of R&B was based on a trend analysis of the ratio IE(XO)/IE(HOX) for X = F, Cl, and Br. From that extrapolation, a range of values of IE(IO), 9.29−9.38 eV, was derived that are 0.36−0.45 eV lower than the experimental value, $\mathrm{IE(IO)} = 9.73_5$ eV, reported here. In light of the general anomalous behavior of FO, as discussed above, the present reevaluation of this trend analysis excludes FO. In addition, we employ the PIMS value for the IE(BrO) of 10.46 eV[28a] (rather than the photoelectron spectroscopy value of 10.29 eV,[46] for reasons discussed previously[28a]) and the recommended value for IE(ClO) of 10.95 eV[36,47] (rather than the preliminary value of 10.87 eV[48]). The values for IE(HOCl) and IE(HOBr) are given in Table 3, and we also employ the recent experimental value for IE(HOI) of 9.81 eV.[27] With these values for IE(ClO) and IE(BrO), the IE(XO)/IE(HOX) ratios are essentially constant with an average value of 0.984_5. This leads to an estimated value for IE(IO) of 9.66 eV, which is in reasonably good agreement with the experimental value determined in the present study, $\mathrm{IE(IO)} = 9.73_5 \pm 0.01_7$ eV. This improvement in agreement between estimated and experimental results (compared to the R&B

derivation[26]) is probably due to the use, here, of more appropriate input values for IE(XO) and IE(HOX).

Thermochemistry. As mentioned in the Introduction, an accurate value for the heat of formation of IO is important in understanding the combustion and atmospheric chemistry of iodine species. However, the range of reported values for $\Delta_f H°_0$(IO) is remarkably wide, from about 109 to 177 kJ mol^{-1}.[17−25] This highlights the large uncertainty surrounding the heat of formation of IO and demonstrates why the thermochemistry of IO remains ambiguous. The value for $\Delta_f H°_0$(IO), 128 ± 4 kJ mol^{-1}, listed in Table 2 was derived from a selected value[8] for $D°_0$(IO), 226 kJ mol^{-1}, that is the average of those from two molecular beam studies.[24,25] The selected value for $D°_0$(IO) appears to fit the $D°_0$(X−O) trend fairly well, apart from the anomalous behavior of FO (which may be expected). It is slightly higher than the bond dissociation energy of CF_3−I[49] and this suggests that reaction 2 is exothermic by about

$$O(^3P) + CF_3I \rightarrow CF_3 + IO \qquad (2)$$

5 kJ mol^{-1}. On the other hand, this $D°_0$(IO) value is lower than that calculated for the C−I bonds in alkyl iodides, for example C_2H_5−I ($D°_0$ = 233 kJ mol^{-1}),[50] so that reaction 5a is

$$O(^3P) + C_2H_5I \rightarrow C_2H_5 + IO \qquad (5a)$$

about 7 kJ mol^{-1} endothermic. This is consistent with the observed dominance[27,51] of the reaction channel leading to HOI

$$O(^3P) + C_2H_5I \rightarrow C_2H_4 + HOI \qquad (5b)$$

which is exothermic by more than 200 kJ mol^{-1}.[52] The selected value of $\Delta_f H°_0$(IO), 128 kJ mol^{-1}, may be used to derive an estimate of the heat of reaction for IO + ClO that is slightly exothermic at ≈4 kJ mol^{-1}. Thus, this reaction cannot be rejected on thermodynamic grounds, in contrast to the conclusion based on $D°_0$(IO) = 209 kJ mol^{-1} ($\Delta_f H°_0$(IO) = 145 kJ mol^{-1}).

Finally, by using the selected value for $D°_0$(IO), 226 kJ mol^{-1}, we can estimate values for $\Delta_f H°_0$(HOI) and the proton affinity (PA) for IO. The trend in $D°_0$(HOX)/$D°_0$(XO) leads to an estimated value of −42.7 kJ mol^{-1} for $\Delta_f H°_0$(HOI).[53] From this result and IE(HOI), 9.81_1 ± 0.020 eV,[27] we compute the heat of formation of HOI^+ at 0 K to be 904 ± 5 kJ mol^{-1}. With the standard value for $\Delta_f H°_0(H^+)$ = 1528 kJ mol^{-1},[36] PA(IO) is readily evaluated by using eq 6 to obtain PA_0(IO) =

$$PA_0(IO) = \Delta_f H°_0(IO) + \Delta_f H°_0(H^+) - \Delta_f H°_0(HOI^+) \qquad (6)$$

752 ± 10 kJ mol^{-1}. There are no experimental values for either $\Delta_f H°_0$(HOI) or PA(IO) with which to compare these estimates.

Acknowledgment. The authors wish to thank Dr. M. Krauss for helpful discussions and for providing results of calculations on the excited states of IO^+ prior to publication. Z.Z. was supported under the Laboratory Directed Research and Development Program at Brookhaven National Laboratory. The work at GSFC was supported by the NASA Upper Atmosphere Research Program. P.S.M. would like to thank the NAS/NRC for the award of a Research Associateship. J.F.L. would like to thank the Chemical Science and Technology Laboratory of the National Institute of Standards and Technology for partial support of his research. The work at BNL was supported by the Chemical Sciences Division, Office of Basic Energy Sciences, U.S. Department of Energy, under Contract DE-AC02-76CH00016. Mention of manufacturers and brand names is to provide a complete description of the apparatus and does not imply endorsement by the National Institute of Standards and Technology or that the items are the best available for their purpose.

References and Notes

(1) Solomon, S.; Garcia, R. R.; Ravishankara, A. R. *J. Geophys. Res.* **1994**, *99*, 20491.

(2) Solomon, S.; Burkholder, J. B.; Ravishankara, A. R.; Garcia, R. R. *J. Geophys. Res.* **1994**, *99*, 20929.

(3) Hamis, A.; Gmurczyk, G.; Grosshandler, W.; Rehwolt, R. G.; Vazquez, I.; Cleary, T.; Presser, C.; Seshadri, K. In *Evaluation of Alternative In-Flight Fire Suppressants for Full-Scale Testing in Simulated Aircraft Engine Nacelles and Dry Bays*; Grosshandler, W. L., Gann, R. G., Pitts, W. M., Eds.; NIST Special Publication 861; 1994; Chapter 4, pp 345−465 and references therein.

(4) Nyden, M. R.; Linteris, G. T.; Burgess, D. F. R.; Westmorland, P. R.; Tsang, W.; Zachariah, M. R. In *Evaluation of Alternative In-Flight Fire Suppressants for Full-Scale Testing in Simulated Aircraft Engine Nacelles and Dry Bays*; Grosshandler, W. L., Gann, R. G., Pitts, W. M., Eds.; NIST Special Publication 861; 1994; Chapter 5, pp 467−641 and references therein.

(5) (a) Battin-Leclerc, F.; Côme, G. M.; Baronnet, F. *Combust. Flame* **1994**, *99*, 644. (b) Hamis, A.; Trees, D.; Seshadri, K.; Chelliah, H. K. *Combust. Flame* **1994**, *99*, 221.

(6) (a) Jenkin, M. E. The photochemistry of iodine-containing compounds in the marine boundary layer. AEA Environment and Energy Report AEA-EE-0405, U.K. (b) Jenkin, M. E.; Cox, R. A.; Candelhand, D. E. *J. Atmos. Chem.* **1985**, *2*, 359.

(7) Babushok, V.; Noto, T.; Burgess, D. R. F.; Hamins, A.; Tsang, W., personal communication, manuscript in preparation.

(8) (a) Huie, R. E. Atmospheric Chemistry of Iodine Compounds. *Prepr. Pap.* (*Am. Chem. Soc., Div. Environ. Chem.*) **1994**, *34*, 736 and references therein. (b) Huie, R. E.; Laszlo, B. In Halon Replacements: Technology and Science. *Adv. Chem. Ser.*, in press.

(9) (a) Clyne, M. A. A.; Watson, R. T. *J. Chem. Soc., Faraday Trans. 1* **1974**, *70*, 1109. (b) Maguin, F.; Mellonki, A.; Laverdet, G.; Poulet, G.; LeBras, G. *Int. J. Chem. Kinet.* **1991**, *23*, 237. (c) Maguin, F.; Laverdet, G.; LeBras, G.; Poulet, G. *J. Phys. Chem.* **1992**, *96*, 1775.

(10) Slagle, I.; Kalinovski, I. J.; Gutman, D.; Harding, L. B. *J. Phys. Chem.*, submitted.

(11) Gilles, M. K.; Turnipseed, A. A.; Rudich, Y.; Talukdar, R. K.; Villalta, P.; Huey, L. G.; Burkholder, J. B.; Ravishankara, A. R., personal communication, to be published.

(12) Vaidya, W. M., *Proc. Indian Acad. Sci. A* **1937**, *6*, 122.

(13) (a) Durie, R. A.; Legay, F.; Ramsay, D. A. *Can. J. Phys.* **1960**, *38*, 444. (b) Carrington, A.; Dyer, P. N.; Levy, D. H. *J. Chem. Phys.* **1970**, *52*, 309. (c) Brown, J. M.; Byfleet, C. R.; Howard, B. J.; Russell, D. K. *Mol. Phys.* **1972**, *23*, 457.

(14) Saito, S. *J. Mol. Spectrosc.* **1973**, *48*, 530 and references therein.

(15) (a) Loewenschuss, A.; Miller, J. C.; Andrews, L. *J. Mol. Spectrosc.* **1980**, *80*, 351. (b) Bekooy, J. P.; Meerts, W. L.; Dymanus, A. *J. Mol. Spectrosc.* **1983**, *102*, 320.

(16) (a) Gilles, M. K.; Polak, M. L.; Lineberger, W. C. *J. Chem. Phys.* **1991**, *95*, 4723. (b) Gilles, M. K.; Polak, M. L.; Lineberger, W. C. *J. Chem. Phys.* **1992**, *96*, 8012.

(17) Coleman, E. H.; Gaydon, A. G.; Vaidya, W. M. *Nature* **1948**, *162*, 108.

(18) Durie, R. A.; Ramsay, D. A. *Can. J. Phys.* **1958**, *36*, 35.

(19) Phillips, L. F.; Sugden, T. M. *Trans. Faraday Soc.* **1961**, *57*, 914.

(20) Gaydon, A. G. *Dissociation Energies*, 3rd ed.; Chapman and Hall: London, 1968.

(21) Rao, M. L. P.; Rao, D. V. K.; Rao, P. T. *Phys. Lett.* **1974**, *50A*, 341.

(22) Trivedi, V. M.; Gobel, V. B. *J. Phys. B* **1972**, *L38*, 5.

(23) (a) Reddy, R. R.; Rao, T. V. R.; Reddy, A. S. R. *Indian J. Pure App. Phys.* **1989**, *27*, 243. (b) It should be noted that Reddy, Rao, and Reddy report a value for D_e(IO) from which the zero point energy, 0.042 eV, must be subtracted to obtain D_0(IO).

(24) Radlein, D. St. A. G.; Whitehead, J. C.; Grice, R. *Nature*, **1975**, *253*, 37.

(25) Buss, R. J.; Sibener, S. J.; Lee, Y. T. *J. Phys. Chem.* **1983**, *87*, 4840.

(26) Ruscic, B.; Berkowitz, J. *J. Chem. Phys.* **1994**, *101*, 7795.

(27) Monks, P. S.; Stief, L. J.; Tardy, D. C.; Liebman, J. F.; Zhang, Z.; Kuo, S.-C.; Klemm, R. B. *J. Phys. Chem.* **1995**, *99*, 16566.

(28) (a) Monks, P. S.; Stief, L. J.; Krauss, M.; Kuo, S. C.; Klemm, R. B. *Chem. Phys. Lett.* **1993**, *211*, 416. (b) Zhang, Z.; Kuo, S.-C.; Klemm, R. B.; Monks, P. S.; Stief, L. J. *Chem. Phys. Lett.* **1994**, *229*, 377.

(29) Nesbitt, F. L.; Marston, G.; Stief, L. J.; Wickramaaratchi, M. A.; Tao, W.; Klemm, R. B. *J. Phys. Chem.* **1991**, *95*, 7613.

(30) Tao, W.; Klemm, R. B.; Nesbitt, F. L.; Stief, L. J. *J. Phys. Chem.* **1992**, *96*, 104.

(31) Kuo, S.-C.; Zhang, Z.; Klemm, R. B.; Liebman, J. F.; Stief, L. J.; Nesbitt, F. L. *J. Phys. Chem.* **1994**, *98*, 4026.
(32) Buckley, T. J.; Johnson, R. D., III; Huie, R. E.; Zhang, Z.; Kuo, S.-C.; Klemm, R. B. *J. Phys. Chem.* **1995**, *99*, 4879.
(33) Grover, J. R.; Walters, E. A.; Newman, J. K.; White, M. C. *J. Am. Chem. Soc.* **1985**, *107*, 7329 and references therein.
(34) Atkinson, R.; Baulch, D. L.; Cox, R. A.; Hampson, Jr., R. F.; Kerr, J. A.; Troe, J. *J. Phys. Chem. Ref. Data* **1992**, *21*, Suppl. No. 4.
(35) Addison, M. C.; Donovan, R. J.; Garraway, J. *Faraday Discuss. Chem. Soc.* **1979**, 286.
(36) Lias, S. G.; Bartmess, J. E.; Liebman, J. F.; Holmes, J. L.; Levin, R. D.; Mallard, W. G. *J. Phys. Chem. Ref. Data* **1988**, *17*, Suppl. No. 1.
(37) The value for IE(I), recommended by Lias et al.,[36] is based upon (a) an optical spectroscopy study: Minnhagen, L. *Ark. Fys.* **1961**, *21*, 415. (b) A photoelectron spectroscopy experiment: Imre, D.; Koenig, T. *Chem. Phys. Lett.* **1980**, *73*, 62.
(38) Kvaran, A.; Yencha, A. J.; Kela D. K.; Donovan, R. J.; Hopkirk, A. *Chem. Phys. Lett.* **1991**, *179*, 263.
(39) Huber, K. P.; Herzberg, G. In *Molecular Spectra and Molecular Structure: IV Constants of Diatomic Molecules*; Van Nostrand Reinhold Co.: New York, 1979.
(40) Krauss, M., personal communication.
(41) Gurvich, L. V.; Veyts, I. V.; Alcock, C. B. *Thermodynamic Properties of Individual Substances*, 4th ed.; Hemispheric Publishing Corp.; New York, 1991; Vol. 2.
(42) Lias, S. G.; Liebman, J. F.; Levin, R. D.; Kafafi, S. A. Positive Ion Energetics. Version 2.0, NIST Standard Reference Database 19A, Gaithersburg, MD, 1993.
(43) Kahr, D.; Yencha, A. J.; Donovan, R. J.; Kvaran, A; Hopkirk, A. *Org. Mass. Spectrosc.* **1993**, *28*, 327.
(44) Monks, P. S.; Stief, L. J.; Krauss, M.; Kuo, S. C.; Klemm, R. B. *J. Chem. Phys.* **1994**, *100*, 1902.
(45) Ruscic, B.; Berkowitz, J. *J. Chem. Phys.* **1994**, *101*, 9215.
(46) Dunlavey, S. J.; Dyke, J. M.; Morris, A. *Chem. Phys. Lett.* **1978**, *53*, 382.
(47) Bulgin, D. K.; Dyke, J. M.; Jonathan, N.; Morris, A. *J. Chem. Soc., Faraday Trans. 2* **1979**, *75*, 456.
(48) Bulgin, D. K.; Dyke, J. M.; Jonathan, N.; Morris, A. *Mol. Phys.* **1976**, *32*, 1487.
(49) (a) Ahonkhai, S. I.; Whittle, E. *Int. J. Chem. Kinet.* **1984**, *16*, 543. (b) Felder, P. *Chem. Phys. Lett.* **1992**, *197*, 425.
(50) Stein, S. E.; Rukkers, J. M.; Brown, R. M. Structures and Properties, Version 1.2, National Institute of Standards and Technology, Gaithersburg, MD, 1991.
(51) Klaassen, J. J.; Lindner, J. L.; Leone, S. R., personal communication, to be published.
(52) The enthalpy of reaction 5b at 298 K may be computed from known or estimated values: $\Delta_f H°_{298}(O) = 249.2$ kJ mol^{-1};[41] $\Delta_f H°_{298}(C_2H_5I) = -9.2$ kJ mol^{-1};[42,50] $\Delta_f H°_{298}(C_2H_4) = 52.4$ kJ mol^{-1};[41] and $\Delta_f H°_{298}(HOI) \approx -46$ kJ mol^{-1} (ref 53 and assuming a correction of about -3 kJ mol^{-1} in converting from 0 to 298 K). The result is $\Delta_r H°_{298} = -234$ kJ mol^{-1} for reaction 5b.
(53) Excluding the anomalous case of X = F, we compute $D°_0(HOX)/D°_0(XO)$ for X = Cl and Br to be 0.8723 and 0.8543 (from thermodynamic values given in ref 41 and, for HOBr, from an average of values in ref 26, ref 44, and McGrath and Rowland (*J. Phys. Chem.* **1994**, *98*, 4773) we obtain $D°_0(HO-Br) = 197.6$ kJ mol^{-1}). Assuming a linear relation for the bond energy trend,[54] the extrapolation to 0.8363 is obtained for $D°_0(HOI)/D°_0(IO)$ and thus $D°_0(HOI) = 189$ kJ mol^{-1} and $\Delta_f H°_0(HOI) = -42.7$ kJ mol^{-1} (ref 27) with an estimated uncertainty of ± 2.5 kJ mol^{-1}.
(54) Steele, W. V. *J. Chem. Thermodyn.* **1978**, *10*, 445; *Ibid.* **1979**, *11*, 187.

JP952405P